Deep-Sea Research, Vol. 36, No. 3, pp. 431–453, 1989.
Printed in Great Britain.

0198-0149/89 $3.00 + 0.00

Remote sensing of oceanic primary production: computations using a spectral model

SHUBHA SATHYENDRANATH,*† TREVOR PLATT,‡ CARLA M. CAVERHILL,‡
RODERICK E. WARNOCK† and MARLON R. LEWIS†

(*Received* 16 *February* 1988; *in revised form* 4 *October* 1988; *accepted* 26 *October* 1988)

Abstract—A spectral model of underwater irradiance is coupled with a spectral version of the photosynthesis–light relationship to compute oceanic primary production. The results are shown to be significantly different from those obtained using the conventional non-spectral approach. The problem of non-uniform vertical distribution of biomass is investigated next, from the point of view of estimation of water-column primary production using satellite data. The errors in estimated production are shown to be functions of parameters of the biomass distribution; of the photosynthesis parameters; and of the optical properties of the water column. Some examples are given to illustrate the comparison of model results with the observed data.

INTRODUCTION

ALTHOUGH the algorithms for estimation of phytoplankton pigments from remotely sensed data are based necessarily on changes in spectral reflectance, most existing methods of analysis do not take into account the interaction of wavelength-dependent optics with the shape of the vertical pigment profile (but see SATHYENDRANATH, 1981; SATHYENDRANATH *et al.*, 1983; SATHYENDRANATH and PLATT, 1989a). Similarly, the methods that have been proposed so far for extraction of information on primary production from ocean colour images have ignored the variation with wavelength of irradiance absorption and utilization by phytoplankton (PLATT, 1986; PLATT *et al.*, 1988; but see PLATT and SATHYENDRANATH, 1988). Here, we evaluate the potential errors in estimation of water-column primary production from available light incurred by not allowing for the spectral character of the relevant processes. Next, we analyse the consequences of nonuniformity in the vertical pigment profile. Finally, we assess the importance of preserving the spectral form of incident radiation in calculation of primary production from remotely sensed data. We show that, in some circumstances, ignoring spectral effects can lead to large errors.

THE MODEL

Light

The light incident at the sea surface, and its subsequent penetration into the interior are modelled according to SATHYENDRANATH and PLATT (1988). This model estimates the

* National Institute of Oceanography, Dona Paula, 403 004 Goa, India.
† Dalhousie University, Halifax, Nova Scotia, Canada B3H 4J1.
‡ Biological Oceanography Division, Bedford Institute of Oceanography, Box 1006, Dartmouth, Nova Scotia, Canada B2Y 4A2.

direct sunlight and the diffuse sky light components of irradiance at the sea surface using the clear-sky transmittance model of BIRD (1984). Fresnel refectance at the sea surface is computed assuming uniformly diffuse sky light and a flat sea surface. Penetration is computed separately for the direct and diffuse components, disregarding multiple scattering effects. At any depth z, the total downwelling irradiance at wavelength λ, $I(z, \lambda)$ (E h^{-1} m^{-2}), is given by

$$I(z,\lambda) = I_d(z, \lambda) + I_s(z, \lambda), \tag{1}$$

where the subscripts d and s refer to the direct sun and diffuse sky components, respectively. The vertical attenuation coefficient for downwelling direct or diffuse irradiance at depth z and wavelength λ, $K(z,\lambda)$ (m^{-1}), is approximated as

$$K(z,\lambda) = \frac{a(z,\lambda) + b_b(z, \lambda)}{\mu}, \tag{2}$$

where $a(z, \lambda)$ is the absorption coefficient (m^{-1}) at depth z, $b_b(z,\lambda)$ is the backscattering coefficient (m^{-1}) at depth z, and μ is the mean pathlength of the light rays per unit vertical excursion. When attenuation is computed for direct sunlight, the parameter μ takes the value of cos θ, where θ is the sun zenith angle in water. It is equal to 0.83 for the sky light component (for uniformly diffuse sky light, 0.83 is the mean value of the cosine of all angles averaged over the cone of refraction, assuming refraction at a flat sea surface). The absorption coefficient is computed as

$$a(z,\lambda) = a_w(\lambda) + a_c^*(\lambda)\, C(z) + a_y^*(\lambda)\, Y(z), \tag{3}$$

where $a_w(\lambda)$ is the partial absorption coefficient due to pure seawater (m^{-1}), $a_c^*(\lambda)$ is the specific absorption coefficient of phytoplankton with associated detritus (m^{-1} (mg m^{-3})$^{-1}$), $C(z)$ is the concentration of phytoplankton and associated detritus at depth z, estimated here as the sum of the concentrations of chlorophyll *a* and phaeopigments (mg m^{-3}), $a_y^*(\lambda)$ is the specific absorption coefficient of dissolved organic matter (dimensionless), and $Y(z)$ is the concentration of dissolved organic matter, expressed in terms of its absorption coefficient at 440 nm (m^{-1}). We have computed $a(z,\lambda)$ according to PRIEUR and SATHYENDRANATH (1981).

In a similar manner, the backscattering coefficient is expressed as

$$b_b(z,\lambda) = b_{bw}(\lambda) + b_{bc}(z,\lambda), \tag{4}$$

where $b_{bw}(\lambda)$ is the backscattering by pure seawater (m^{-1}), and $b_{bc}(\lambda)$ is the backscattering by phytoplankton (m^{-1}). To compute $b_{bw}(\lambda)$ we have used the results of MOREL (1974). Total scattering by phytoplankton at 550 nm is calculated according to MOREL (1980), and the backscattering computed from it, supposing that the ratio of backscattering to total scattering is 0.5% for phytoplankton. Scattering spectrum of phytoplankton is assumed to have a form that is complementary to the absorption spectrum (MOREL and BRICAUD, 1981; BRICAUD *et al.*, 1983).

It may be noted that equations (3) and (4) assume the concentration of non-chlorophyllous particles to be zero, which is a reasonable assumption for open-ocean waters. Again, as a first approximation for open-ocean waters, absorption by yellow substances may be taken to covary with phytoplankton absorption (PRIEUR and SATHYENDRANATH, 1981). But, in coastal waters where phytoplankton may not be the single

independent variable responsible for changes in the inherent optical properties of the water, an extra term would have to be added to the right-hand side of equations (3) and (4), to account for non-chlorophyllous particles. In such waters, it would also be necessary to compute the absorption by yellow substances independently of phytoplankton concentration.

In the non-spectral irradiance model that is most commonly used in primary production studies, and which is used here for comparison with the spectral model, the parameter of interest is $\bar{K}(z)$ (m^{-1}), the vertical attenuation coefficient for $I(z)$, the total PAR at depth z [photosynthetically active radiation, given by the integral of $I(z,\lambda)$ from 400 to 700 nm]. It is generally expressed as

$$\bar{K}(z) = \bar{K}_w + C(z)\bar{k}_c + \bar{K}_x(z), \tag{5}$$

where $\bar{K}_w$ (m^{-1}) is the attenuation coefficient due to pure seawater, $\bar{k}_c$ (m^{-1} (mg m^{-3})$^{-1}$) is the effective specific attenuation coefficient of phytoplankton and $\bar{K}_x$ (m^{-1}) is the contribution to attenuation from other substances (suspended sediments or dissolved organic matter). The parameters $\bar{K}_w$ and $\bar{k}_c$ are assumed to be invariant with depth.

Primary production

Neglecting photoinhibition, the dependence of photosynthesis on available light can be expressed by an equation containing two parameters (PLATT *et al.*, 1977). The parameters most commonly chosen are the initial slope α^B (mg C (mg Chl *a*)$^{-1}$ (E m^{-2})$^{-1}$) and the assimilation number P_m^B (mg C (mg Chl *a*)$^{-1}$ h^{-1}) where the superscripts B indicate normalization to pigment biomass. All of the photosynthesis–light models in the literature can be written in terms of these two parameters, with little to choose between the various alternatives (PLATT *et al.*, 1977, 1988). Here we use the equation of SMITH (1936):

$$P(z) = \frac{P_m^B(z)\ B(z)\ \{I(z)/I_k(z)\}}{[1 + \{I(z)/I_k(z)\}^2]^{1/2}}, \tag{6}$$

where $P(z)$ is primary production at depth z (mg C m^{-3} h^{-1}), $I(z)$ is photosynthetically active radiation (PAR) (E h^{-1} m^{-2}) at depth z, $B(z)$ is chlorophyll *a* concentration (mg m^{-3}) at depth z. Note that B is not identical to C. The variable C includes phaeopigments which contribute to light attenuation, but B accounts for only the photosynthetically active Chl *a*. The parameter P_m^B is the assimilation number (mg C (mg Chl *a*)$^{-1}$ h^{-1}), α^B is the initial slope (mg C (mg Chl *a*)$^{-1}$ (E m^{-2})$^{-1}$) and I_k is the adaptation parameter (E $m^{-2}h^{-1}$), defined as P_m^B/α^B. Notice that the adaptation parameter is a derived parameter, not a further independent parameter. Equation (6), the conventional form of the photosynthesis-light relation in which the spectral and angular distributions of light are suppressed, has to be considered no more than an approximation to reality.

In passing to a spectral form of equation (6) (SATHYENDRANATH and PLATT, 1989b), the wavelength dependence of the photosynthesis–light parameters has to be considered. The maximum rate of photosynthesis under light-saturating conditions, is generally considered to be independent of wavelength (PICKETT and MYERS, 1966), and in the absence of information to the contrary, we take it to be so. In contrast, α^B, the rate of photosynthesis under light-limiting conditions, is strongly wavelength-dependent. The spectral dependency of α^B is complex by virtue of the fact that it is a function of the independent absorption properties of the two photosystems; their independent quantum yields; and the requirement that both photosystems operate in series. Where the *effective*

spectral absorption properties of the two photosystems are similar, however, effects such as Emerson enchancement may be ignored and a useful approximation is the photosynthetic action spectrum, $\alpha^B(\lambda)$, defined as the light-limited rate of photosynthesis determined in monochromatic light as a function of wavelength (DUYSENS, 1970; LEWIS *et al.*, 1985a,b, 1986). For all oceanic material examined to date, the strong correspondence between this action spectrum and the absorption spectrum (LEWIS *et al.*, 1985b; WARNOCK, unpublished data, see Fig. 1) suggests this is a reasonable approximation (DUYSENS, 1970).

Furthermore, the shape of $\alpha^B(\lambda)$ appears to be strongly conservative between regions, at least according to the limited data available so far (LEWIS *et al.*, 1985b; WARNOCK, unpublished data). This is consistent with, and reinforces the results of PRIEUR and SATHYENDRANATH (1981) on the conservative nature of the shape of $a_c^*(\lambda)$. Here we shall assume that both $a_c^*(\lambda)$ and $\alpha^B(\lambda)$ conserve spectral *form*, but that their *magnitudes* may vary. The spectral forms of $a_c^*(\lambda)$ and $\alpha^B(\lambda)$ used in this study are shown in Fig. 1.

The conventional, non-spectral values of a_c^* and α^B can be related to the spectral values through equations like

$$\alpha = \langle \alpha(\lambda) \rangle_\lambda = \frac{\int \alpha(\lambda) d\lambda}{\int d\lambda} \tag{7a}$$

$$a_c^* = \langle a_c^*(\lambda) \rangle_\lambda = \frac{\int a_c^*(\lambda) d\lambda}{\int d\lambda}, \tag{7b}$$

where the integrals are taken over the photosynthetically active spectrum and the subscript λ indicates averaging with respect to wavelength.

Equation (6) can now be rewritten to include the explicit dependence on the spectral and angular distributions of available light. Replacing I_k with P_m^B/α^B and noting that

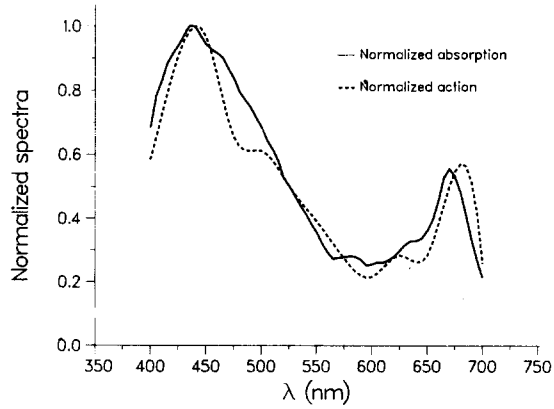

Fig. 1. Action and absorption spectra of phytoplankton, normalized at 440 nm. The absorption spectrum is from PRIEUR and SATHYENDRANATH (1981), based on *in situ* measurements in various oceanic regions. The action spectrum is from WARNOCK (unpublished data). It represents the mean of a large number of observations in the Arctic. The original data is for 12 wavelengths from 400 to 680 nm, and has been interpolated for every 5 nm from 400 to 700 nm to match the absorption spectrum. The extension from 680 to 700 nm is arbitrary.

$\alpha = B\alpha^B$, we have, for normally incident, monochromatic light at wavelength λ,

$$P(z,\lambda) = \alpha(z,\lambda)\, I(z,\lambda) \left[1 + \left(\frac{\alpha(z,\lambda)\, I(z,\lambda)}{P_m}\right)^2\right]^{-\frac{1}{2}}. \tag{8}$$

The formulation in equation (8) is based on the light $I(z,\lambda,\theta)$ which is *available* at depth z. To retain the effect of the angular distribution of the light field we should now consider the light *absorbed*.

The spectral values of the maximum *realised* quantum yield measured using monochromatic illumination, $\phi_m(\lambda)$, has a similar definition to that of $\alpha^B(\lambda)$, but in terms of absorbed light I_a (PLATT, 1986). Thus,

$$\alpha(\lambda) = \left.\frac{dP}{dI(\lambda)}\right|_{I(\lambda)\to 0} \tag{9a}$$

$$\phi_m(\lambda) = \left.\frac{dP}{dI_a(\lambda)}\right|_{I(\lambda)\to 0}. \tag{9b}$$

Note that the maximum realised quantum yield $\phi_m(\lambda)$ obtained in this way is distinct from Φ_m, the maximum theoretical quantum yield possible in a polychromatic light field where the distribution of excitation energy between the two photosystems is optimally balanced and all non-linear processes are taken into account. Consequently, $\phi_m(\lambda)$ will be less than or equal to Φ_m, for all λ. For normally incident light we have

$$\alpha(z,\lambda) = \phi_m(z,\lambda)\, a_c^*(\lambda)\, B(z), \tag{10}$$

where we have selected from the right-hand side of equation (3) the term that corresponds to absorption by photosynthetically active pigments. For a collimated beam passing through the water at zenith angle θ, the effective absorption coefficient per unit vertical distance is higher by a factor sec θ than that for a normally incident beam (equation 2). Hence,

$$\alpha(z,\lambda,\theta) = \phi_m(z,\lambda)\, a_c^*(\lambda)\, B(z) \sec\theta\,. \tag{11}$$

For uniformly diffuse sky light, after refraction at a flat surface, the analagous equation is

$$\alpha(z,\lambda,s) = 1.20\, \phi_m(z,\lambda)\, a_c^*(\lambda)\, B(z), \tag{12}$$

where 1.20 is the reciprocal of the factor 0.83 appearing in equation (2). Clearly, equation (11) applies to the direct component I_d and equation (12) to the sky component I_s of incident light.

Combining equations (8), (10), (11) and (12) and integrating over λ, we find (SATHYENDRANATH and PLATT, 1989b)

$$P(z) = \mathrm{II}(z)/\sqrt{1 + (\mathrm{II}(z)/P_m(z))^2}, \tag{13}$$

where

$$\mathrm{II}(z) = \int \phi_m(z,\lambda) a_c^*(\lambda)\, B(z) \sec\theta\, I_d(z,\lambda,\theta) d\lambda + \int 1.20 \phi_m(z,\lambda) a_c^*(\lambda)\, B(z) I_s(z,\lambda)\, d\lambda. \tag{14}$$

Assuming that the photosynthesis parameters are invariant with depth, and restoring

$\alpha(\lambda)$ in place of $\phi_m(\lambda)\, a_c^*(\lambda)\, B(z)$, we have

$$\Pi(z) = \sec\theta \int \alpha(\lambda) I_d(z,\lambda,\theta)\, d\lambda + 1.20 \int \alpha(\lambda) I_s(z,\lambda)\, d\lambda. \quad (15)$$

Note that the integrals of α over λ are now weighted by the spectral composition of the light field, unlike those in equations (7), which are unweighted wavelength averages.

Deep-sea chlorophyll maximum (DCM)

To the effect of non-uniform biomass distribution in the water column, we use the generalized pigment profile (PLATT *et al.*, 1988) expressed as

$$B(z) = B_0 + \frac{h}{\sigma\sqrt{2\pi}} \exp\left[-\frac{(z - z_m)^2}{2\sigma^2}\right]. \quad (16)$$

Here, B_0 (mg m^{-3}) is the background pigment concentration; σ (m) defines the width of the peak; z_m (m) is the depth of chlorophyll maximum; and h (mg m^{-2}) determines the total biomass above the background. The height of the peak above the baseline is given by $h/(\sigma\sqrt{2\pi})$.

Discussion of the model

The results of the optical model used here are seen to compare well with *in situ*, open-ocean data from the North Atlantic (SATHYENDRANATH and PLATT, 1988). However, the model makes some simplifying assumptions, and it is worth estimating the errors that they imply. The optical model used here assumes that the angular distribution of light is invariant with depth. This is not strictly true, but its variability with depth has been shown to be fairly small (<10%) in clear waters, based on both theoretical considerations and observations (PREISENDORFER, 1959; PRIEUR, 1976; DIRKS and SPITZER, 1987). On the other hand, depth dependence of K (due to changes in the angular distribution of light under water) increases as the water becomes more turbid (KIRK, 1983). We estimate that in our computations, errors in K are maximum for high chlorophyll concentrations, and for the green part of the spectrum. For a chlorophyll concentration of 10 mg m^{-3}, K in the green would be underestimated by 25% at half the euphotic depth (SATHYENDRANATH and PLATT, 1988). Equation (2) assumes that K increases inversely as μ. In fact, upward scattering due to particles would increase faster than $1/\mu$, due to pronounced asymmetry in the shape of the volume scattering function (which defines the angular dependence of scattering). This error is maximum for maximum sun zenith angles and for maximum chlorophyll concentration. To estimate this error, we assumed that the shape of the volume scattering function for particles corresponds to the mean curve given by PETZOLD (1972). Then, for $\theta = 90^0$, and for chlorophyll concentration = 10 mg m^{-3}, the error in K would be 3.8% at 440 nm, and 9.3% at 550 nm. Again, the error in K is seen to be maximum in the green, which corresponds to the minima in phytoplankton absorption and action spectra. Consequently, the effect of these errors on estimated primary production would be minimal.

COMPARISON OF THE SPECTRAL MODEL WITH THE NON-SPECTRAL MODEL

The absorption and scattering properties of pure seawater and those of the optically active substances present in it are all wavelength-dependent. The incoming solar

radiation also has a variable spectral form that depends on solar elevation and atmospheric conditions. The spectral quality of light available in the sea is therefore susceptible to changes with depth, water quality and the nature of the incident solar radiation. The absorption and utilization of light by phytoplankton are also wavelength-dependent (Fig. 1). Models of primary production that ignore these wavelength effects are therefore subject to potential errors. In this section, we examine the way errors arise in key parameters of the models from neglect of spectral effects, and calculate their magnitudes in some typical cases.

In the computations presented in this section, $\bar{K}_w$ and $\bar{k}_c$ of equation (5) are assigned values of 0.035 (m^{-1}) and 0.04 (m^{-1} (mg m^{-3})$^{-1}$), respectively. The $a_c^*(\lambda)$ values in equation (3) were scaled such that their mean value was equal to 0.04 (m^{-1} (mg m^{-3})$^{-1}$) (equation 7b). The last terms of both equations (3) and (5) were dropped, to simplify the interpretation of results.

Spectral distribution of light

To demonstrate the spectral composition of irradiance at the sea surface, the computed irradiance spectra for 21 June at the equator are shown in Fig. 2, for every half hour from 0700 to 1200 h (local apparent time). It is clear that there is considerable variation, with changing solar elevation, in the relative importance of diffuse and direct components, and in their respective spectral forms. As a case study, spectral irradiance at the euphotic depth is presented in Fig 3, for the incident irradiance corresponding to 1030 h, in waters with chlorophyll concentrations ranging from 0.01 to 10 (mg m^{-3}). In the calculations, it was supposed that the vertical biomass distribution was uniform. The figure clearly demonstrates the shift in irradiance maximum from blue to green with increasing pigment concentration. This implies that increasing pigment concentrations render the light field progressively more unfavourable for absorption and utilization by phytoplankton, given that both the absorption and action spectra of phytoplankton peak in the blue and are minimum in the green (Fig. 1). The shift in irradiance maximum from blue to green also implies that in chlorophyll-rich waters, attenuation by pure seawater

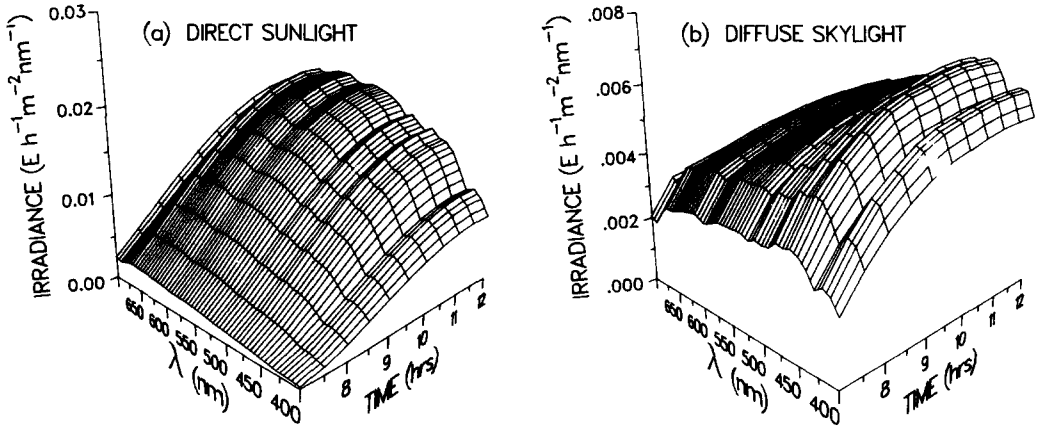

Fig. 2. Spectra of direct and diffuse irradiance at the sea surface, for a hypothetical station at the equator on a clear day, on 21 June. The spectra were computed using the clear-sky model of Bird (1984).

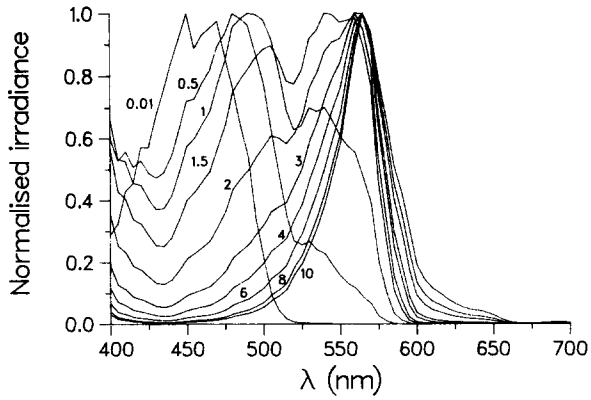

Fig. 3. Computed spectra of total downwelling irradiance at the euphotic depth, for waters with various concentrations of chlorophyll, supposed to be uniform at all depths. The numbers next to each curve represent the chlorophyll concentration in the water column, in mg m^{-3}. The incident irradiance at the surface is assumed to be the same in all cases, and corresponds to that for 1030 h in the previous figure.

will be higher than in chlorophyll-poor water, since pure seawater attenuation in the green is many times higher than in the blue [from SMITH and BAKER (1981), diffuse irradiance attenuation by pure seawater is 0.0168 (m^{-1}) at 450 nm and 0.0717 (m^{-1}) at 565 nm]. A small increase is noted in the irradiance spectra from 440 to 400 nm, for high chlorophyll concentrations. This effect arises from the absorption maximum of chlorophyll at 440 nm. A similar effect is observed in the irradiance spectra for offshore productive waters given by MOREL (1982). We next examine the consequence of these shifting spectral forms in determining the euphotic depth and the primary production of the water column.

Euphotic depth

According to equation (5), the euphotic depth z_p is given by

$$z_p = \frac{4.6}{\bar{K}_w + C\bar{k}^c} \tag{17}$$

for the uniform biomass case considered here, and when $\bar{K}_x$ is neglected. This means that $1/z_p$ is a linear function of C, with slope $\bar{k}_c/4.6$ and intercept $\bar{K}_w/4.6$. When spectral effects are taken into account, however, such a simple relationship no longer holds, since $\bar{K}_w$ and $\bar{k}_c$ are functions of depth, water quality and solar elevation (SATHYENDRANATH and PLATT, 1988). In Fig. 4a, we have plotted $1/z_p$ as a function of C. Also plotted is the $1/z_p$ curve computed using the spectral model for the same incident light field as in Fig. 3. The spectrally derived curve shows pronounced non-linearity for low pigment concentrations, and the euphotic depth is generally lower than that obtained from the non-spectral model (the difference between the two estimates of euphotic depth ranges from –15 to +46%). Another point to bear in mind is that the euphotic depth, in the spectral model, is also sensitive to solar elevation, since μ intervenes in the equation for attenuation. The diurnal variation in euphotic depth is plotted in Fig. 4b, for a water column with uniform pigment concentration of 1 (mg m^{-3}). The euphotic zone deepens by about 20%

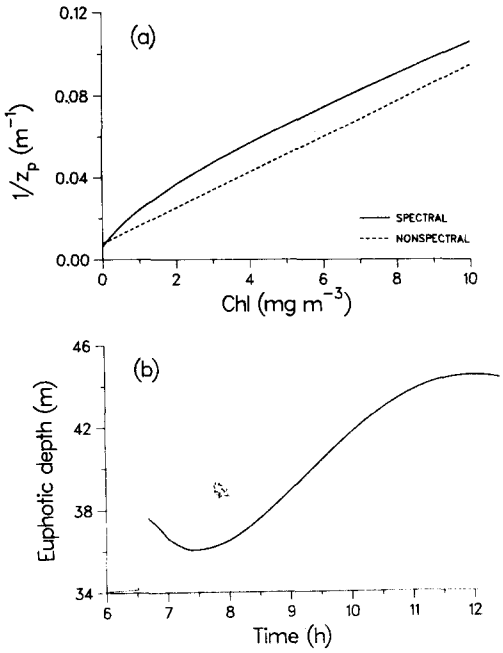

Fig. 4. (a) Computed values of the reciprocal of the euphotic depth z_p (m^{-1}) as a function of chlorophyll *a* concentration in the water column. The incident irradiance is the same as for the previous figure. Also plotted is an analytical solution to the nonspectral model ($1/z_p = \bar{K}_w/4.6 + Ck_c/4.6$, with $\bar{K}_w = 0.035$ m^{-1} and $k_c = 0.04$ m^{-1} (mg m^{-3})$^{-1}$). (b) Time dependence of the euphotic depth (z_m). The computed curve represents the values from early morning to noon, for a water column with chlorophyll concentration of 1 (mg m^{-3}). For the incident irradiance, see Fig. 2.

from morning to noon. Note that the minimum does not occur at lowest zenith angle, but about half an hour later. This is due to changes in the spectral quality of the incident light and in the relative importance of direct and diffuse light, which counteract the effect of increasing solar elevation. It is well known that the angular distribution of underwater light changes progressively, and trends to an asymptotic distribution at great depth (PREISENDORFER, 1959; TYLER, 1960). This distribution is independent of the angular distribution of the incident light, and is determined only by the inherent optical properties of the water. JERLOV (1976) has reported that asymptotic distribution may not be reached at 100 m or even at 400 m, depending on the water type and the wavelength involved. KIRK (1983) has computed that for fairly turbid waters, asymptotic distribution is reached at the base of the euphotic zone. The depth dependence of angular distribution is not accounted for in our model, and the tendency towards asymptotic distribution would decrease the time dependence seen in Fig. 4b. However, we expect this effect to be small, since angular distribution over a major part of the euphotic zone is strongly dependent on the distribution of incident light, even when the tendency towards asymptotic distribution is taken into account.

Fractional light absorption by phytoplankton

In the non-spectral model, the fraction of incident light that is absorbed by

phytoplankton, S, may be computed as

$$S = \frac{\bar{k}_c B}{\bar{K}_w + \bar{K}_x + \bar{k}_c B} \tag{18}$$

again, for the case of uniform biomass distribution (PLATT, 1986). Therefore, when $\bar{K}_x$ is neglected, $S/(1 - S)$ is a linear function of C, with slope $\bar{k}_c/\bar{K}_w$ and zero intercept. Note that $S/(1 - S)$ is the ratio of phytoplankton absorption to background absorption. This ratio was computed for the spectral model, and is plotted as a function of C in Fig. 5. The linear, non-spectral relationship is also plotted. The result of the spectral model shows pronounced non-linearity, with phytoplankton absorption efficiency decreasing as the concentration increases. This is another consequence of the changing spectral quality of the underwater light field.

Water-column production

In the case of the non-spectral model, the exact solution for the column-integrated production ($\int_z P$) for uniform biomass distribution is given by

$$\int_z P = (P_m/\bar{K})\log_e[I_* + \sqrt{1 + I_*^2}] \tag{19}$$

(PLATT, 1986, equation 22), where $I_* = I(0)/I_k$. The parameter P_m in this equation is not normalized to biomass. Daily integrated primary production, computed using equation (19) is plotted in Fig. 6a as a function of chlorophyll concentration. In these computations, phaeopigment concentration was assumed to be zero. In other words, C and B

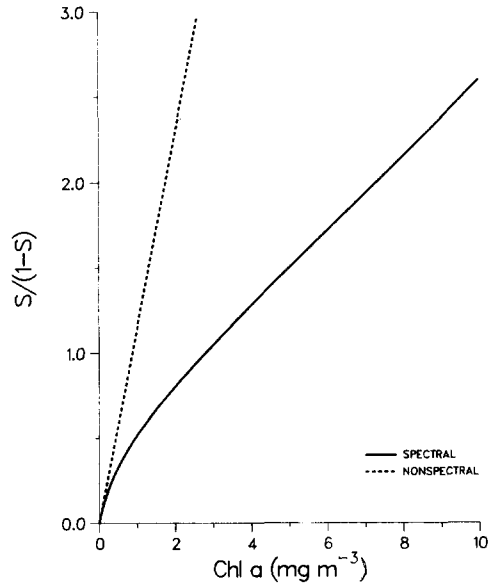

Fig. 5. Phytoplankton absorption of available light, as a function of chlorophyll concentration in the water column. The parameter S is the fraction of available light (daily) that is absorbed by phytoplankton. Therefore, $S/(1 - S)$ is the ratio of phytoplankton absorption to the background absorption. Computations are for the equator, on 21 June. Also plotted is a linear solution to the non-spectral model ($S/(1 - S) = C\bar{k}_c/\bar{K}_w$, with same values for $\bar{K}_w$ and $\bar{k}_c$ as in the previous figure).

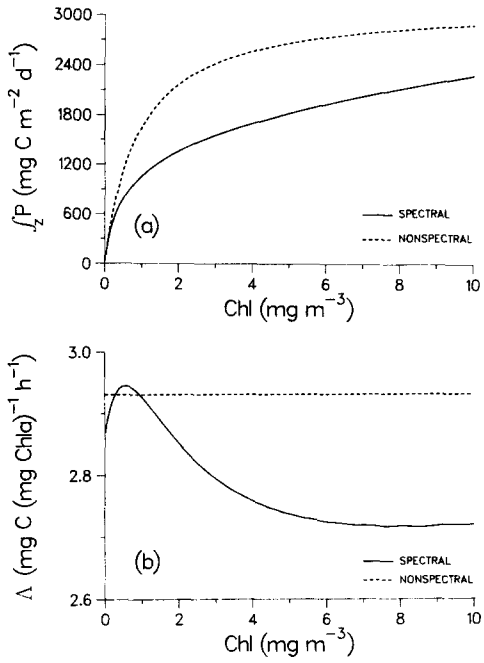

Fig. 6. (a) Daily column-integrated primary production, computed using the spectral and non-spectral models, and plotted as a function of the uniform chlorophyll concentration in the water column. Computations are for P_m^B = 5(mg C (mg Chl *a*)$^{-1}$ h^{-1}) and α^B = 0.1 (mg C (mg Chl *a*)$^{-1}$ h^{-1} (W m^{-2})$^{-1}$). (b) Same as (a), but the total production (per hour) has been normalized to the total chlorophyll in the euphotic zone. $\Lambda = \int_z P/(B\, z_p)$. The solution to the non-spectral model is independent of the chlorophyll concentration in the water column and of the optical properties of the water.

are equivalent. The incident radiation is the same as in Fig. 7e. In this numerical example, P_m^B was assigned the value of 5 (mg C (mg Chl *a*)$^{-1}$ h^{-1}) and α^B, 0.1 (mg C (mg Chl *a*)$^{-1}$ h^{-1} (W m^{-2})$^{-1}$). [The values of α^B are given here in units of Watts merely to facilitate comparison with PLATT *et al.* (1988). In the computations, Watts were converted to quanta using the relationship of MOREL and SMITH (1974): 1 W m^{-2} = 2.77 × 10^{18} quanta m^{-2} s^{-1}, and quanta to Einsteins using the relationship 1 E = 6.022 × 10^{23} quanta.]

Water-column production up to the base of the euphotic zone was also computed numerically, using the spectral model. The values of $\alpha^B(\lambda)$ were normalized such that the mean of the spectral values was the same as the value of α used in the non-spectral model (according to equation 7a). Compared to the spectral model, the non-spectral model underestimates production slightly (by 6%) for low values of chlorophyll concentration, and overestimates it at high concentrations (the overestimate may be as high as 60%). This is easily understood when we consider that the spectrally weighted α will be greater than the mean in the blue waters that favour phytoplankton absorption, whereas the opposite would be true in green waters. It is also seen that the non-spectral production curve reaches saturation at lower chlorophyll concentrations than does the spectral version. This may be attributed, in the spectral model, to the increasing background

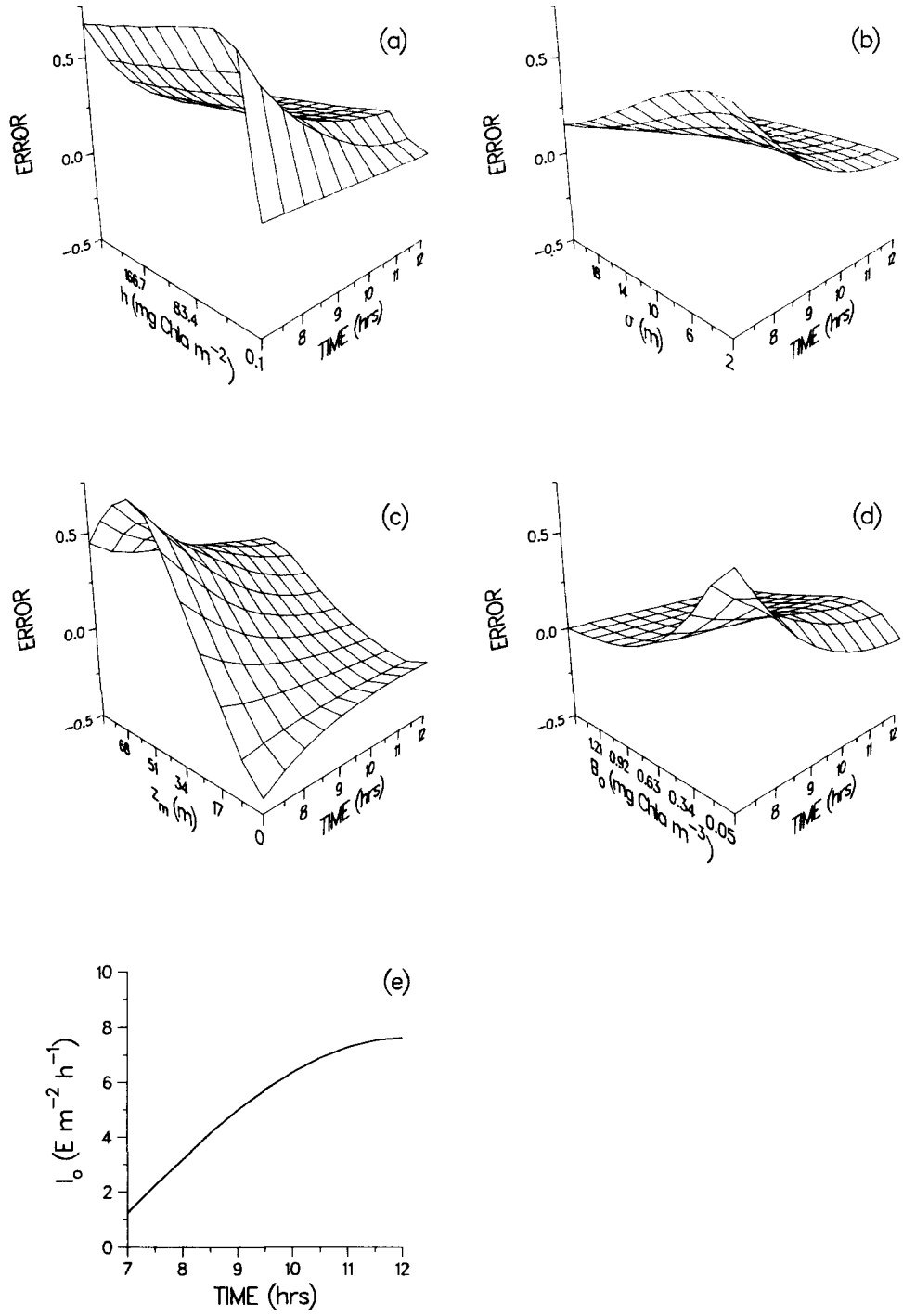

Fig. 7. (a–d) Relative error in computed production (Method I) as a function of the four parameters of the chlorophyll profile, and of time of day. When one of the parameters is being varied, the others revert to their typical values. The incident spectra at the sea surface are given in Fig. 2, and the total irradiance is given in (e).

attenuation with increasing pigment concentration, arising from shift in shape of spectrum of available light.

The spectral effect is also significant in determining the value of Λ, defined as the water-column production normalized to the total biomass in the euphotic zone (PLATT, 1986; PLATT *et al.*, 1988). For uniform biomass distribution, the total biomass in the euphotic zone is given by Bz_p. With $z_p = 4.6/\bar{K}$, the analytical expression for Λ in the non-spectral model can be derived from equation (19) as

$$\Lambda = (P_m/4.6)\log_e[I_* + \sqrt{1 + I_*^2}] \,. \tag{20}$$

According to equation (20), Λ does not depend on the optical properties of the water, but only on the incident radiation and the photosynthetic parameters P_m and α. Values of Λ, computed for the spectral and non-spectral cases, are plotted in Fig. 6b. Incident radiation was kept constant, with PAR equal to 6.9 (E h^{-1} m^{-2}) (which corresponds to the computed incident irradiance at 1030 h in Fig. 2). Otherwise, the parameters computed are the same as in Fig. 6b. Unlike the non-spectral model, the Λ values computed using the spectral model are not independent of the water quality. We find that the spectral Λ is slightly greater (by 0.5%) than the non-spectral estimate for some chlorophyll-poor waters, and lower in chlorophyll-rich waters by up to 8%. Again, this may be attributed to the fact that the weighted average of α would be greater than its mean in blue waters but less than the mean in green waters. Another important point is that, due to the high absorption of red light by pure seawater, attenuation of light by the water itself is very high at the surface where light availability is maximal (SATHYENDRANATH and PLATT, 1988). This also contributes to the decreased light utilization by phytoplankton as seen in the spectral model.

CONSEQUENCE OF NON-UNIFORM BIOMASS DISTRIBUTION

Details of the vertical pigment distribution are not always available for use in computation of primary production. It is then usual to make the simplifying assumption that the pigments are distributed uniformly in the water column. In other words, it is assumed that the pigment distribution is characterized by a single (known) quantity.

Using a non-spectral model of light penetration and primary production, PLATT *et al.* (1988) investigated the potential errors in estimated production that ensue from this assumption. Various non-uniform pigment profile types were generated by changing the four parameters of the generalized pigment profile (equation 16). Sensitivity of the errors to the four parameters of the pigment profile, to the two photosynthetic parameters and to two optical parameters of the water were investigated. Two methods were used in their study. In Method I, it was assumed that the known quantity is the mean concentration of chlorophyll in the euphotic zone. In Method II, it was assumed that the known quantity is the satellite-weighted surface chlorophyll. The approach used here is identical to that just outlined (PLATT *et al.*, 1988), except for the use of the spectral model.

Sensitivity analyses were carried out around a typical profile defined by the following parameters: h = 18.8 (mg Chl *a* m^{-2}), σ = 5 m, z_m = 42.5 m and B_0 = 0.1 (mg Chl *a* m^{-3}). The parameter P_m^B is assigned a value of 5 (mg C (mg Chl *a*)$^{-1}$ h^{-1}), and $\alpha^B(\lambda)$ has a spectral mean of 0.1 (mg C (mg Chl *a*)$^{-1}$ h^{-1} (W m^{-2})$^{-1}$). As in the previous section, B and C are taken to be equivalent, yellow substances and non-chlorophyllous particles are

assumed to be absent (unless stated otherwise), and $a_c^*(\lambda)$ has a mean value of 0.04 (m^{-1} (mg m^{-3})$^{-1}$). The case studies presented here are for hypothetical stations at the equator, on a clear day (21 June, see Fig. 2 for the computed incident irradiance spectra). Relative error in estimated production, Δ, was computed as the difference between the uniform and non-uniform cases, normalized to the non-uniform case (positive error means that assumption of uniform distribution leads to over-estimate in production). Sensitivity of the errors to changes in the various parameters is discussed next.

Method I

Parameters of the generalized pigment profile. To study the sensitivity of relative error Δ to changes in h, σ, z_m and B_0, these parameters were varied one by one, over a range of plausible values, and the error computed in each case. The relative errors in hourly production are presented in Fig. 7a – d as a function of time, from early morning to noon. Dependence of the error on time comes mainly through changing *magnitude* of incident irradiance (see Fig 2 for the spectra of direct and diffuse downwelling irradiance at the surface, and Fig. 7e for total downwelling PAR). Maximum errors, equal to about 70%, are observed in the early morning. The errors generally decrease with increasing surface irradiance (with the exception of very small or very large values of z_m), though the rate of decrease is variable depending on the parameter and irradiance values.

Daily integral. The errors in daily integral of production, as a function of the parameters of the biomass profile are shown in Fig. 8. Maximum relative errors are less than 40%. For h, σ and B_0, an initial increase in the parameter values leads to an increase in error, but the trend reverses for high parameter values. The shape of the error curve and its range are different for the different parameters. The error appears to be most sensitive to the parameter z_m. It increases steadily with increasing z_m, until z_m approaches 70 m (close to the euphotic depth), after which it begins to decrease.

The parameters P_m^B *and* α^B. Increasing P_m^B or decreasing α^B leads to an increase in the error (Fig. 9). The error decreases from morning to noon in the examples studied here.

Method II

In this method, the satellite-weighted surface chlorophyll is computed according to GORDON and CLARK (1980) (see also PLATT *et al.*, 1988). The weighted surface concentration is then assumed to be representative of the whole water column.

Parameters of the pigment profile. Relative error in computed production resulting from this method is plotted in Fig. 10 for the same values of h, σ, z_m and B_0 as in Fig. 7. Maximum error in the examples studied here is around 90% and occurs for a chlorophyll maximum at the surface. But for the most part, the errors range between 0 and –50%. Note that, with this method, the maximum errors are at noon, and there is a general reversal of the sign of the errors when compared to Method II. In our results using the non-spectral model (PLATT *et al.*, 1988), the range of errors was lower for Method II than Method I. But with the spectral model, the two methods yield roughly the same range of errors.

Biomass and background absorption. We also investigated the consequences of increased biomass in the water column (or inversely, of increased background absorption by substances other than phytoplankton). Since the error appears to be more sensitive to z_m than to the other parameters, this sensitivity analysis was carried out for different values of z_m. However, changing the optical properties also altered the euphotic depth.

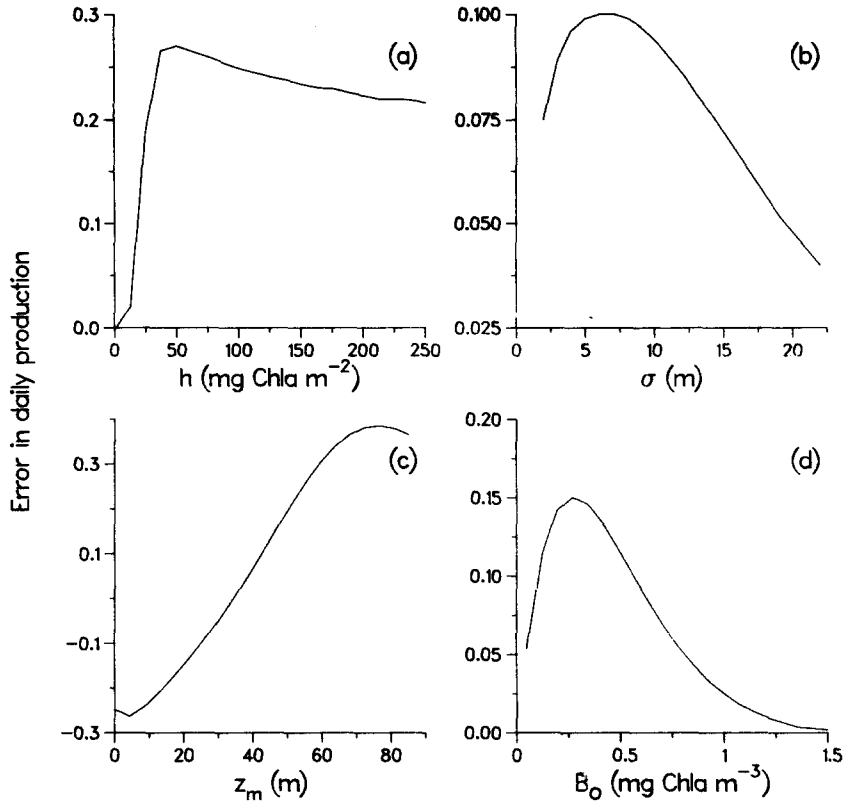

Fig. 8. Error in daily integrated production (Method I), for the same parameter values as in the previous figure.

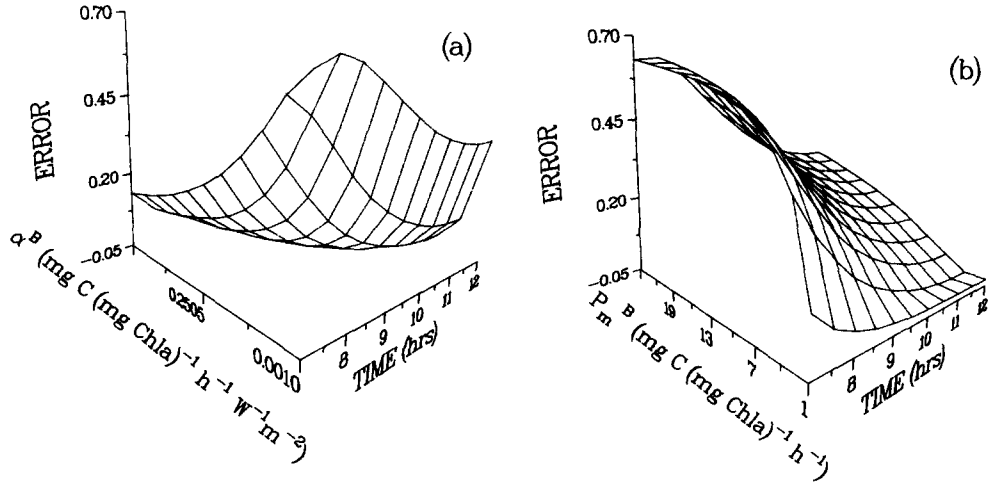

Fig. 9. Relative error in computed production (Method I) for various values of the photosynthetic parameters α^B and P_m^B. The profile parameters are held constant at their typical values.

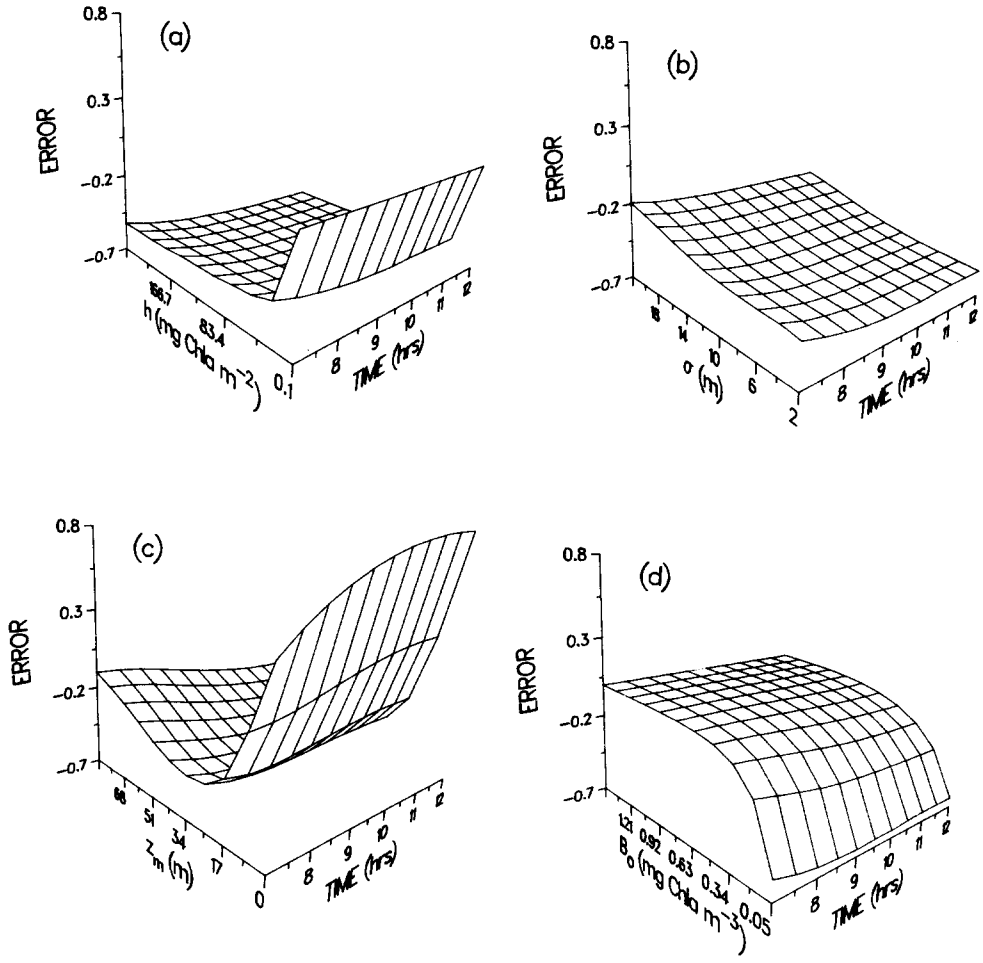

Fig. 10. Relative error in computed production, same as Fig. 7, but using Method II.

The range of z_m was therefore scaled in each case such that most of the z_m values studied lay within the euphotic zone.

The error curves in Fig. 11a and b represent the cases where the biomass at each depth has been multiplied by two and four, respectively, compared to the typical curves used in the previous figure. In Fig. 11c and d, the biomass is the same as for the corresponding cases in Fig. 10, but absorption by yellow substances and non-chlorophyllous particles has been introduced. Concentration of non-chlorophyllous particles, measured in terms of increased scattering at 550 nm, is assumed to be 1(m^{-1}) in Fig. 11c and 2(m^{-1}) in Fig. 11d. Absorption by yellow substances amounts to 20% of total absorption at 440 nm, in both Fig. 11c and d. Spectral absorption by non-chlorophyllous particles and yellow substances is modelled according to PRIEUR and SATHYENDRANATH (1981). The scattering by non-chlorophyllous particles is assumed to vary inversely with wavelength, and the scattering-to-backscattering ratio of these particles is assumed to be 1%. Figure 11 shows that increased biomass results in a decrease in the range of errors, whereas increased

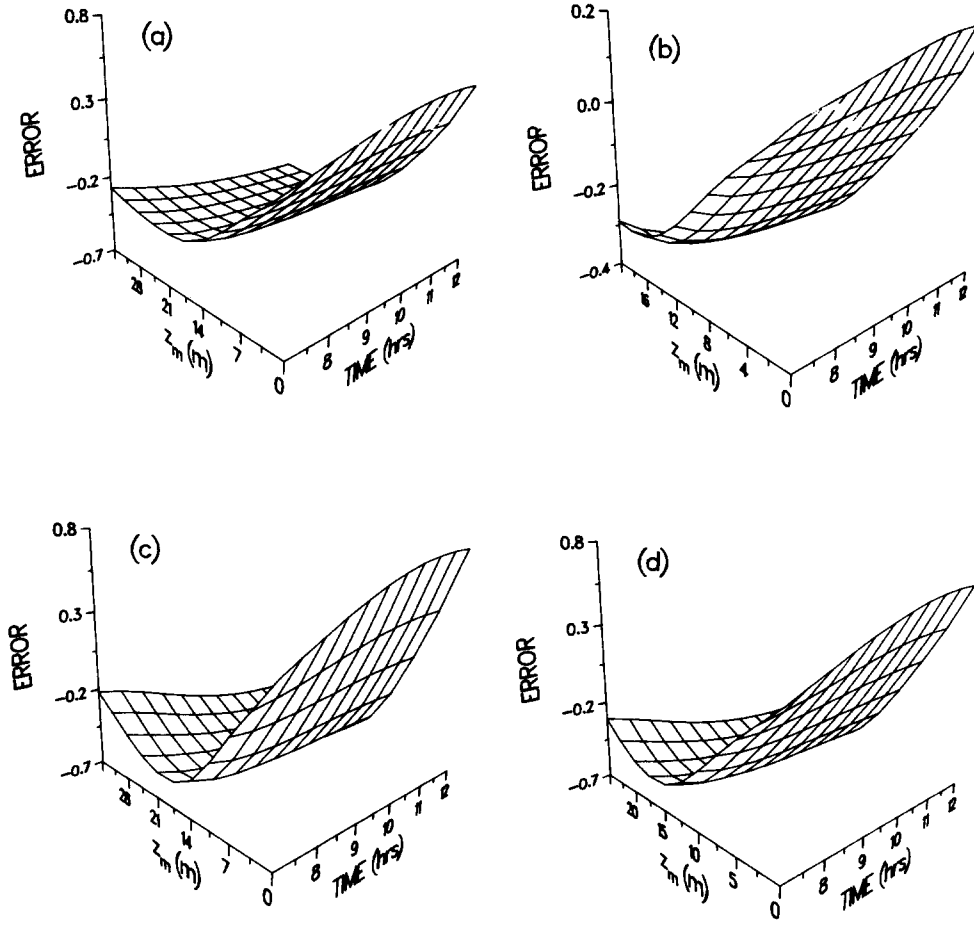

Fig. 11. Effect of changing biomass and background absorption on the relative error in estimated production (Method II). (a, b) Biomass has been increased. The sensitivity analysis is carried out around typical profiles where the parameters h and B_0 have been multiplied by a factor x. For (a), $x = 2$, and for (b), $x = 4$. (c, d) Biomass is held constant ($x = 1$), while absorption by non-chlorophyllous particles and dissolved organic matter has been added. The concentration of non-chlorophyllous particles in (d) is twice that in (c). In both (c) and (d), absorption by yellow substances is put to 20% of total absorption at 440 nm.

background absorption increases the range of errors. Note however, that the positive error for a chlorophyll maximum at the surface is slightly reduced when background absorption increases.

The spectral quality of incident light

It has been shown in an earlier section that estimated primary production is sensitive to spectral changes in underwater light. But how much of it is due to changes in the incident-light spectra? To examine this question, a sensitivity analysis was carried out in which production was re-computed assuming that the incident diffuse and direct irradiances both had flat spectra. The error arising from this assumption is plotted in Fig. 12 for different parameter values. The results show that the error may be as high as

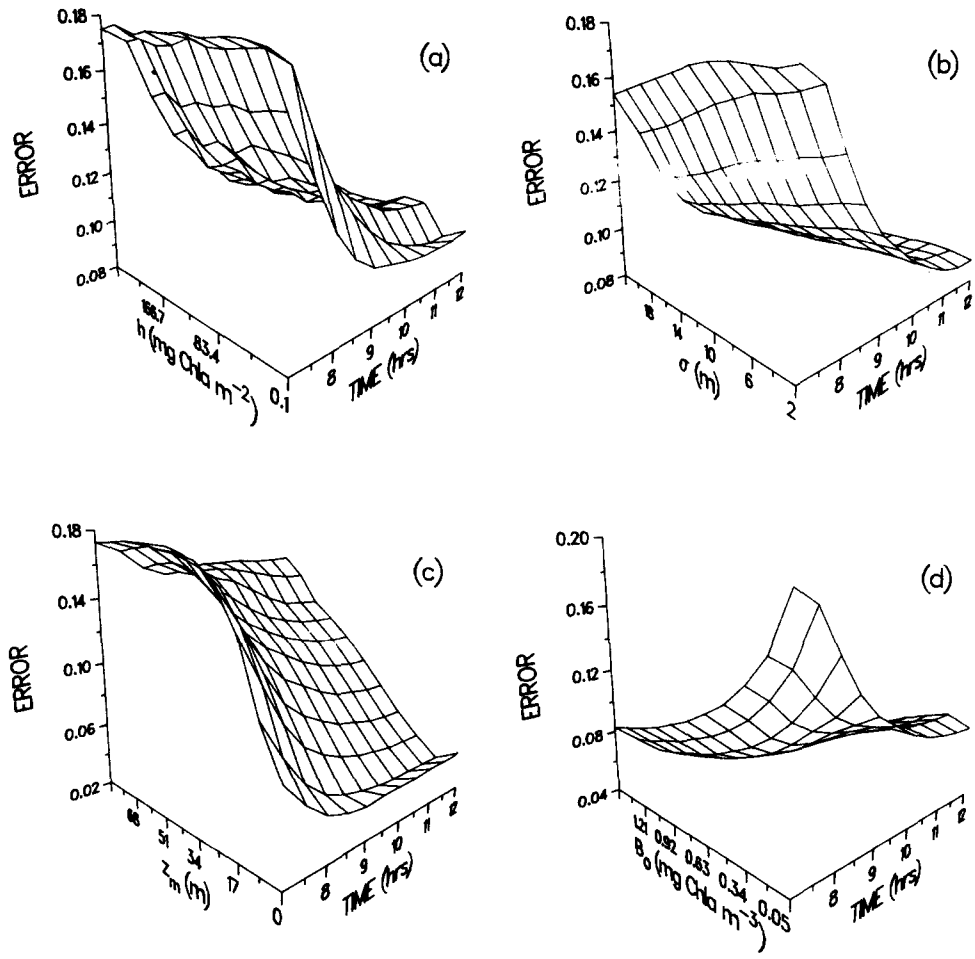

Fig. 12. Error in estimated production when the spectral form of the incident spectrum is neglected, plotted as a function of time and parameter values.

17% for some of the parameter values, or as low as 5%. The spectral form of incident radiation is therefore not a detail that can be safely disregarded.

Discussion of the error curves

PLATT *et al.* (1988) explained the error curves, plotted as a function of I_*, in terms of four dimensionless factors: (1) the depth of the DCM relative to the euphotic depth, (2) the width of the peak relative to the euphotic depth, (3) the ratio of peak height to background, and (4) the ratio of background absorption to phytoplankton absorption. We found that their results from the simple non-spectral model could, in fact, be used to explain the complex behaviour of the error curves of the spectral model used in this study. Generally, the error curves from this model follow the same pattern as those of the non-spectral model, and the same arguments seem to hold true. The major difference is in the magnitudes of the errors: they are smaller in the case of the spectral model. Note also, that in this model, the euphotic depth varies with time of day. Therefore some

ambiguity exists in the definition of the first two dimensionless factors, unless their time-dependence is suppressed. In the non-spectral model, $\bar{K}_w$ and $\bar{k}_c$ are constant with depth. A consequence is that the euphotic depth is not sensitive to the depth of the biomass peak (z_m), as long as the entire peak remains within the photic zone. This is no longer true in the spectral model, since the optical properties of the water are depth-dependent. This dependence of z_p on z_m adds to the complexity of scaling the parameters to the euphotic depth.

COMPARISON OF MODEL RESULTS WITH DATA

Measured biomass profiles

The sensitivity analysis on generalized pigment profiles presented here has shown that neglecting non-uniformity in the biomass profile can lead to significant errors in estimated production. It is however, difficult to make an exhaustive study of all possible combinations of the parameters involved, given the large number of parameters and the complex manner in which they interact. It is also possible that some of the combinations of parameters may not be representative of natural conditions. To estimate the errors that may be expected in real cases, we subjected a large number of observed chlorophyll profiles from various regions to an error analysis. Whenever measurements of photosynthetic parameters were available, representative values of α^B and P_m^B were assigned to the data from that locality. When they were not available, as in the case of the Indian Ocean data, these parameters were assigned values of 0.1 (mg C (mg Chl a)$^{-1}$ h^{-1} (W m^{-2})$^{-1}$) and 5 (mg C (mg Chl a)$^{-1}$ h^{-1}), respectively. In the sensitivity analysis, and in the comparison of the spectral model with the non-spectral model, the mean spectral value of a_c^* was held constant, to facilitate interpretation of results. However, according to PRIEUR and SATHYENDRANATH (1981), there is reason to suppose that the specific absorption coefficient is higher in oligotrophic waters than in phytoplankton-rich waters. For this analysis, therefore, we used the relationship

$$a_c^*(440) = \frac{0.355}{6.103 + C} \tag{21}$$

(SATHYENDRANATH and PLATT, 1988). In the absence of data on the concentration of non-chlorophyllous particles, their concentration was put to zero, but absorption by yellow substances was assumed to contribute 20% to the total absorption at 440 nm (a reasonable assumption for open-ocean waters, according to the results of PRIEUR and SATHYENDRANATH, 1981).

Errors were computed using both Methods I and II, and are presented in Fig. 13a and b as a function of chlorophyll concentration (mean as well as satellite-weighted). These results obtained using actual profiles show maximum errors (of the order of 70%) for waters with low chlorophyll concentrations, falling off rapidly with increasing concentrations. The errors are generally less than ±10% for mean chlorophyll concentrations greater than 5(mg m^{-3}) or lie between 0 and −20% for the same satellite-weighted concentrations. Most of the errors are positive for Method I and negative for Method II, a consequence of the fact that deep chlorophyll maxima are more common in these data sets than surface maxima. Another interesting point is that the data from a given location tend to group together, suggesting that it may be possible, at least in certain instances, to characterize oceanic regions on the basis of their profile parameters.

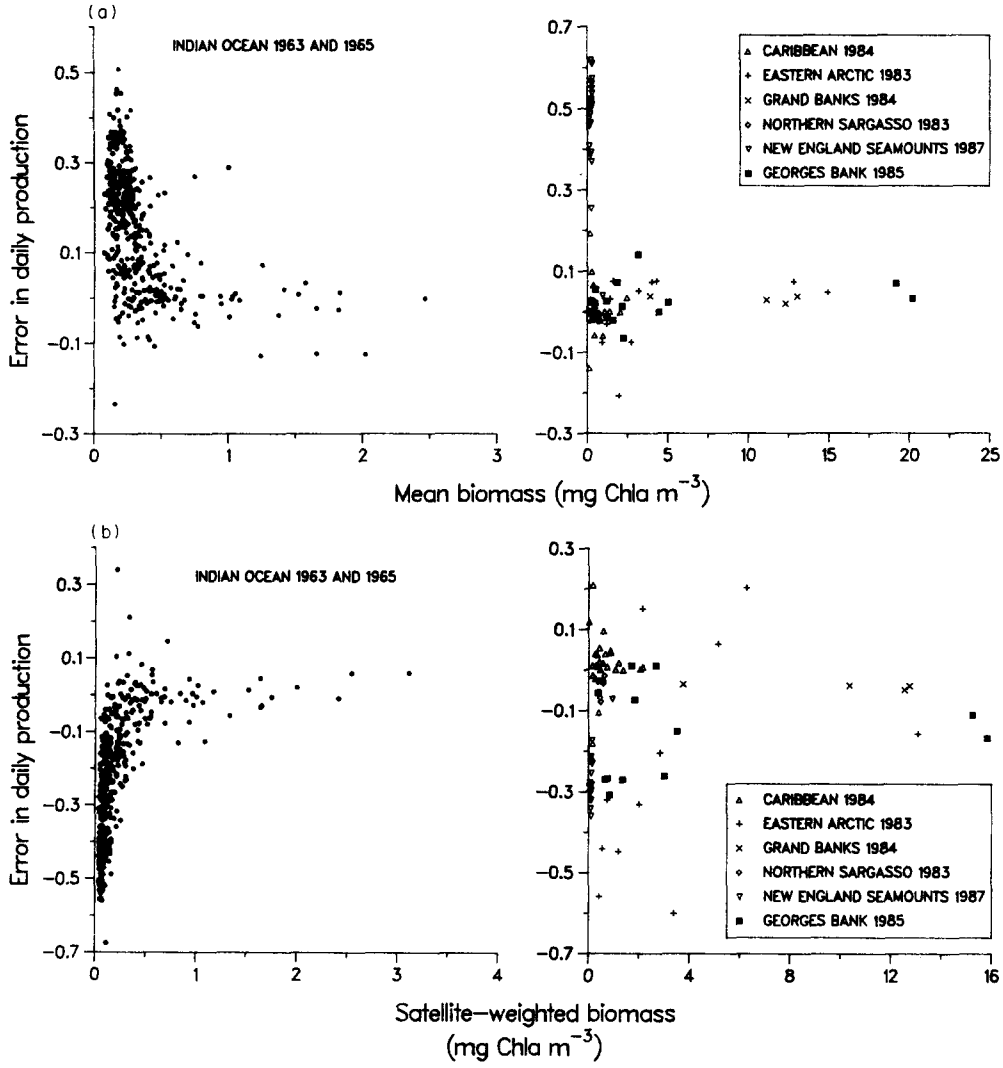

Fig. 13. Error in daily integrated primary production, for observed *in situ* profiles. (a) Method I, (b) Method II. Error is plotted as a function of the chlorophyll concentration expressed as the euphotic-zone mean or the satellite-weighted surface value.

Primary production

Primary production estimated with the spectral model used here was compared against measured production at 31 stations in the North Atlantic (PLATT and SATHYENDRANATH, 1988). The computations were based on measured profiles of chlorophyll and phaeophytin at each station. The agreement was excellent, with slope not significantly different from unity, intercept not significantly different from zero, and 95% of the variance explained (with one outlier excluded). This is a particularly encouraging result, considering that no effort was made to adjust the optical parameters to suit local conditions, and that each locality was assigned just one set of P_m^B and α^B values, instead of individual values for each station. For cases where the stations were occupied during

very cloudy weather (11 out of the 31), the limitation of the *clear-sky* model for surface irradiance could not be ignored. It was found that, for a rough correction, it was sufficient to scale the estimated production by the ratio of measured daily irradiance to the estimated clear-sky irradiance.

CONCLUSIONS

A clear picture is now beginning to emerge of the potential capabilities and limitations of the physiological approach to the problem of remote sensing of phytoplankton productivity (PLATT and SATHYENDRANATH, 1988). The proposed approach consists of estimating photosynthetically available radiation at the sea surface as well as the satellite-weighted surface chlorophyll concentration by remote sensing. Supplementary information to be supplied based on *in situ* measurements would be the parameters of the pigment profile, the photosynthetic parameters and the optical properties of the water column. Note, however, that the passive fluorescence technique offers some possibility of estimating one of the photosynthetic parameters, the initial slope α^B, by remote sensing (TOPLISS and PLATT, 1986).

This study has shown that the results from our spectral model are significantly different from those of a conventional non-spectral model. A need therefore exists to emphasize studies based on the spectral dependence of light penetration and photosynthesis in the ocean, rather than on mean properties for the total photosynthetically active radiation.

Our studies also show that the results are sensitive to changes in the spectral quality of incident light. This poses a problem, because the techniques presently available for remote sensing of downwelling irradiance at the sea surface yield only total short-wave irradiance (GAUTIER and KATSAROS, 1984). Clear-sky transmittance models like that of BIRD (1984) used in this work can be used to study the spectral and angular distribution under cloudless skies, but the results would not be so satisfactory on cloudy days, since clouds alter not only the total amount of radiation at the sea surface, but its spectral form as well. Since cloud optics depend on the type, quantity and spatial distribution of clouds, there appears to be no simple solution to the problem of computing spectral irradiance under cloudy skies. But the model of PINKER and EWING (1985) does give a decomposition of the visible spectrum into three spectral regions, which is at least a start.

It might be argued that the need for supplementary information on *in situ* properties nullifies the usefulness of remote sensing. This would be true if those parameters that are not amenable to remote sensing were not stable over large horizontal distances and with time. The approach that appears most promising therefore is to measure the rapidly changing variables (chlorophyll, light) through remote sensing and supplement the data by *in situ* measurements of the stable parameters. This combination of measurements should yield a more complete picture of the large-scale variability of biological productivity than would be possible using either method by itself (PLATT and SATHYENDRANATH, 1988). Though there is reason to believe that the chlorophyll profile parameters and the optical and photosynthetic parameters are quasi-stable properties of oceanic regions, there is a paucity of such data to prove the case for many localities. Classification of oceanic regions based on their bio-optical parameter values appears to be a necessary step to the full exploitation of the potentialities of remote sensing.

Acknowledgements—This work was supported by a grant-in-aid from the Department of Ocean Development (New Delhi) to NIO (Goa). The necessary collaboration was greatly facilitated by the award of an NSERC(Canada) International Scientific Exchange Fellowship to SS. Further NSERC support through Operating Grants to MRL and TP is gratefully acknowledged.

REFERENCES

BIRD R. E. (1984) A simple, solar spectral model for direct-normal and diffuse horizontal irradiance. *Solar Energy*, **32**, 461–471.

BRICAUD A., A. MOREL and L. PRIEUR (1983) Optical efficiency factors of some phytoplankters. *Limnology and Oceanography*, **28**, 816–832.

DIRKS R. W. J. and D. SPITZER (1987) Solar radiance distribution in deep natural waters including fluorescence effects. *Applied Optics*, **26**, 2427–2430.

DUYSENS L. N. M. (1970) Photobiological principles and methods. In: *Photobiology of microorganisms*, P. HALLDAL, editor, Wiley-Interscience, New York, pp. 1–16.

GAUTIER C. and K. B. KATSAROS (1984) Insolation during STREX: comparisons between surface measurements and satellite estimates. *Journal of Geophysical Research*, **89**, 11,779–11,788.

GORDON H. R. and D. K. CLARK (1980) Remote sensing of optical properties of a stratified ocean: an improved interpretation. *Applied Optics*, **19**, 3428–3430.

JERLOV N. G. (1976) *Marine optics*. Elsevier, Amsterdam, 231pp.

KIRK J. T. O. (1983) *Light and photosynthesis in aquatic ecosystems*. Cambridge University Press, Cambridge, 401 pp.

LEWIS M. R., R. E. WARNOCK and T. PLATT (1985a) Absorption and photosynthetic action spectra for natural phytoplankton populations: implications for production in the open ocean. *Limnology and Oceanography*, **30**, 794–806.

LEWIS M. R., R. E. WARNOCK, B. IRWIN and T. PLATT (1985b) Measuring photosynthetic action spectra of natural phytoplankton populations. *Journal of Phycology*, **21**, 310–315.

LEWIS M. R., R. E. WARNOCK and T. PLATT (1986) Photosynthetic response of marine picoplankton at low photon flux. In: *Photosynthetic picoplankton*, T. PLATT and W. K. W. LI, editors, *Canadian Bulletin of Fisheries and Aquatic Sciences*, **214**, 235–250.

MOREL A. (1974) Optical properties of pure seawater. In: *Optical aspects of oceanography*, N. G. JERLOV and E. STEEMANN NIELSEN, editors, Academic, London, pp. 1–24.

MOREL A. (1980) In-water and remote measurememts of ocean color. *Boundary-Layer Meteorology*, **18**, 177–201.

MOREL A. (1982) Optical properties and radiant energy in the waters of the Guinea Dome and the Mauritanian upwelling area in relation to primary production. *Rapports et Procès-verbaux des Réunions. Conseil Permanent International pour l'Exploration de la Mer*, **180**, 94–107.

MOREL A. and R. C. SMITH (1974) Relation between total quanta and total energy for aquatic photosystems. *Limnology and Oceanography*, **19**, 591–600.

MOREL A. and A. BRICAUD (1981) Theoretical results concerning optics of phytoplankton with a special reference to remote sensing applications. In: *Oceanography from space*, J. F. R. GOWER, editor, Plenum, New York, pp. 313–327.

PETZOLD (1972) Volume scattering functions for selected ocean waters. San Diego: Scripps Inst. Oceanogr., Ref 72–78, 79pp.

PICKETT J. M. and J. MYERS (1966) Monochromatic light saturation curves for photosynthesis in *Chlorella*. *Plant Physiology*, **41**, 90–98.

PINKER R. T. and J. A. EWING (1985) Modeling surface solar radiation: Formulation and validation. *Journal of climate and Applied Meteorology*, **24**, 389–401.

PLATT T. (1986) Primary production of the ocean water column as a function of surface light intensity: algorithms for remote sensing. *Deep-Sea Research*, **33**, 149–163.

PLATT T., K. L. DENMAN and A. D. JASSBY (1977) Modelling the productivity of phytoplankton. In: *The sea: ideas and observations on progress in the study of the seas*, Vol. 6, E. D. GOLDBERG, I. N. MCCAVE, J. J. O'BRIEN and J. H. STEELE, editors, Wiley-Interscience, pp. 807–856.

PLATT T. and S. SATHYENDRANATH (1988) Oceanic primary production: estimation by remote sensing at local and regional scales. *Science*, **241**, 1613–1620.

PLATT T., S. SATHYENDRANATH, C. CAVERHILL and M. R. LEWIS (1988) Ocean primary production and available light: further algorithms for remote sensing. *Deep-Sea Research*, **35**, 855–879.

PREISENDORFER R. W. (1959) Theoretical proof of the existence of characteristic diffuse light in natural waters. *Journal of Marine Research*, **18**, 1–9.

PRIEUR L. (1976) Transfer radiatif dans les eaux de la mer. Doctorat D'Etat, Univ. P. & M. Curie, 243 pp.

PRIEUR L. and S. SATHYENDRANATH (1981) An optical classification of coastal and oceanic waters based on the specific spectral absorption curves of phytoplankton pigments, dissolved organic matter, and other particulate materials. *Limnology and Oceanography*, **26**, 671–689.

SATHYENDRANATH S. (1981) Influence des substances en solution et en suspension dans les eaux de mer sur l'absorption et la réflectance. Modélisation et application à la télédétection. Doctorat 3e Cycle, Université Paris VI, 123 pp.

SATHYENDRANATH S. and T. PLATT (1988) The spectral irradiance field at the surface and in the interior of the ocean: a model for applications in oceanography and remote sensing. *Journal of Geophysical Research*, **93**, 9270–9280.

SATHYENDRANATH S. and T. PLATT (1989a) Remote sensing of ocean chlorophyll: consequence of non-uniform pigment profile. *Applied Optics*, in press.

SATHYENDRANATH S. and T. PLATT (1989b) Computation of aquatic primary production: extended formalism to include effect of angular and spectral distribution of light. *Limnology and Oceanography*, in press.

SATHYENDRANATH S., L. PRIEUR and A. MOREL (1983) Rapport complémentaire. Contrat ESA 4726-81-F. DD.SC, 29 pp.

SMITH E. L. (1936) Photosynthesis in relation to light and carbon dioxide. *Proceedings of the National Academy of Sciences*, **22**, 504–511.

SMITH R. C. and K. S. BAKER (1981) Optical properties of the clearest natural waters (200–800 nm). *Applied Optics*, **20**, 177–184.

TOPLISS B. J. and T. PLATT (1986) Passive fluorescence and photosynthesis in the ocean: implications for remote sensing. *Deep-Sea Research*, **33**, 849–864.

TYLER J. E. (1960) Radiance distribution as a function of depth in an underwater environment. *Bulletin of the Scripps Institution of Oceanography*, **7**, 363–411.